Multiscale and Multidisciplinary Modeling, Experiments and Design (2024) 7:2507–2514
https://doi.org/10.1007/s41939-023-00348-5

ORIGINAL PAPER

Microscopic insight into the effect of particle gradation on the dynamic compaction of dry sand using DEM

Yuqi Li[1] · Liangchen Xu[1] · Fu'an Yang[1]

Received: 6 October 2023 / Accepted: 13 December 2023 / Published online: 20 January 2024

Abstract
Particle gradation is an important feature of granular materials, which has a significant influence on the mechanical properties of soil. Several dynamic compaction (DC) tests for mono-sized dry sand samples and a well-graded dry sand sample were modeled using discrete element method. The effect of particle gradation on crater depth was analyzed as well as coordination number, porosity and contact stress from a microscopic view. It is indicated that the change rates of dynamic stress, coordination number and porosity of the well-graded sample were greater than the results from the mono-sized samples. For the mono-sized samples and the well-graded sample, the differences in dynamic contact stress, coordination number and porosity became larger as the distance of measurement point from ground surface increased. The results also demonstrate from a microscopic view that the well-graded soil and the mono-sized soil with smaller particle size were more prone to become dense under DC. This study at a grain level is helpful to understand the microscopic mechanism of DC and has a certain guiding significance to the construction of DC.

Keywords Dynamic compaction · DEM · Particle gradation · Coordination number · Porosity

1 Introduction

When the geological conditions of a construction site are poor, it is usually necessary to carry out foundation treatment on the site. Dynamic compaction (DC), as a widely used foundation treatment method, can improve the bearing capacity of foundation and reduce post-construction settlement by converting the gravitational potential energy of a lifted tamper into kinetic energy and acting on the ground in the form of an impact load. It is suitable for a wide variety of soil types, especially sandy soils and coarse granular soils; however, caution is required when used in saturated soils and clayey soils (Lukas 1980; Miao et al. 2006; Ghassemi et al. 2010). Numerous studies on DC have been carried out through analytical solutions, field and laboratory tests and numerical simulation (Chow et al. 1992; Feng et al. 2000; Hu et al. 2001; Gu and Lee 2002; Wang et al. 2017) due to its wide application in ground treatment.

Few analytical solutions of DC to date have been deduced because of complexity of impact contact stress and heterogeneity of foundation soil. Aiming at the limitation of linear spring dashpot dynamic models applied to relatively soft ground, an improved analytical model was proposed and verified through experimental data (Thilakasiri et al. 1996). For a liquefiable soil and soft soil interbedded foundation in highway engineering practice, the in-situ tests for evaluating effectiveness of the lower tamping energy were performed and the formulation of predicting the improvement depth of DC was proposed (Miao et al. 2006).

As for field and laboratory tests, many researchers had done plenty of outstanding work (Mayne et al. 1984; Takada and Oshima 1994; Feng et al. 2000; Hu et al. 2001; Hwang and Tu 2006; Jia et al. 2009). Mayne et al. (1984) studied the relationship between the size of the craters, ground vibration levels, the depth of influence and the level of energy per blow according to the data from more than 120 field tests. Hwang and Tu (2006) analyzed the effects of tamping energy and isolation trench on ground vibration based on the ground vibration data of an industrial site during DC.

✉ Yuqi Li
liyuqi2000@shu.edu.cn

Liangchen Xu
xvliangchen@126.com

Fu'an Yang
1871025949@qq.com

[1] Department of Civil Engineering, Shanghai University, Shanghai, China

Through laboratory DC tests, the influence of pounder base shape on the efficiency of DC (Feng et al. 2000) and the variation of microstructural variation of soils (Hu et al. 2001; Jia et al. 2009) were analyzed. Furthermore, the centrifuge test of DC was also used to simulate an actual foundation treatment project (Takada and Oshima 1994).

Apart from those investigations mentioned above, a lot of studies focused on the numerical modeling of DC (Poran and Rodriguez 1992; Chow et al. 1992; Pan and Selby 2002; Gu and Lee 2002; Lee and Gu 2004; Ghassemi et al. 2010; Xie et al. 2013; Wang et al. 2017). To estimate the degree and depth of improvement resulting from DC, Lee and Gu (2004) proposed a numerical method taking into account momentum, energy, tamper area and the initial state of the ground, Chow et al. (1992) established a one-dimensional wave equation model in conjunction with standard penetration test results, and Wang et al. (2017) deduced a forecasting formulas for ground deformation with comprehensive consideration of soil properties, shape of tamper, energy level, construction method and number of blows. Also, a fully coupled hydro-mechanical finite element code for evaluating DC of saturated granular soil was developed by Ghassemi et al. (2010) and the simulation results were verified by the data from a real field case of DC treatment in a highway. In addition, micro mechanism of DC was studied by using discrete element method (DEM) (Li et al. 2018; Ma et al. 2014; Jiang et al. 2017), in which the improvement effect and the influence depth of DC were analyzed based on the porosity change of the foundation soil (Ma et al. 2014; Jiang et al. 2017), and a centrifuge test of dry sand under DC (Takada and Oshima 1994) was modeled to investigate the microscopic characteristics of sand under DC at a particle level (Li et al. 2021).

These foregoing studies provided many data for design and construction of DC and the influence of gradation on the behavior of soil has also attracted interest of a few researchers (Lu et al. 2013; Luo et al. 2014; Fang et al. 2016; Gu et al. 2017). The effects of the initial particle size and moisture on the compressive behavior of dense sand under high strain rates were investigated by Lu et al. (2013) and Luo et al. (2014). An analysis approach for simulating the mechanical behavior of dry sand under static and dynamic loadings was put forward and applied in the domain of projectile penetration into the sand particulate system, and the effect of particle size on the projectile penetration depth and ballistic instability was further discussed (Fang et al. 2016). By studying the effect of particle size distribution on the small strain shear stiffness of granular soils, Gu et al. (2017) explored the fundamental mechanism controlling this small strain shear stiffness. However, they seldom studied the influence of particle gradation on DC, especially at a grain level. In this paper, in order to assess the effect of particle gradation on DC from a microscopic view, based on DEM (Ma et al. 2014; Jiang et al. 2017; Li et al. 2018; Liu et al. 2020), the DC simulations of sand samples with different grading were conducted, and the dynamic stress, coordination number, porosity and crater depth of soils were thoroughly investigated.

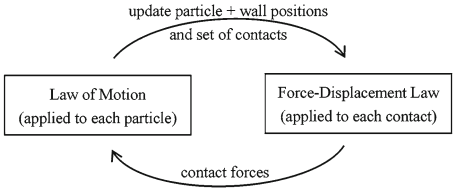

Fig. 1 Calculation cycle in PFC^{2D}

2 Principle of DEM

As a DEM, Particle Flow Code in 2 dimensions (PFC^{2D}) models the movement and interaction of rigid circular particles (Itasca Consulting Group 2004). The calculations performed in PFC^{2D} alternate between the application of Newton's second law to the particles and a force–displacement law at the contacts. Newton's second law is used to determine the motion of each particle arising from the contact and body forces acting on it, while the force–displacement law is used to update the contact forces arising from the relative motion at each contact. In PFC^{2D}, the presence of walls requires only that the force–displacement law accounts for ball-wall contacts. Newton's second law is not applied to walls since the wall motion is specified by users (Itasca Consulting Group 2004). The calculation cycle is illustrated in Fig. 1.

3 Numerical simulations

3.1 Contact constitutive model

The hysteretic damping contact model can reflect energy dissipation by hysteretic damping (Itasca Consulting Group 2004; Jia et al. 2015), so it was selected to simulate the dynamic characteristics of soil during DC in this paper. As shown in Fig. 2 (Itasca Consulting Group 2004), the normal stiffness of the model is different at the loading and unloading stages, and the normal stiffness on loading is smaller than that on unloading in the hysteretic damping model. Used in the hysteretic damping model, the normal stiffnesses on loading, $k_{\mathrm{n\_load}}$, and on unloading, $k_{\mathrm{n\_unload}}$, are calculated using the following equations:

$$k_{\mathrm{n\_load}} = \frac{2R_{\mathrm{h}}k_0}{1+R_{\mathrm{h}}} \tag{1}$$

$$k_{\mathrm{n\_unload}} = \frac{2k_0}{1+R_{\mathrm{h}}}, \tag{2}$$

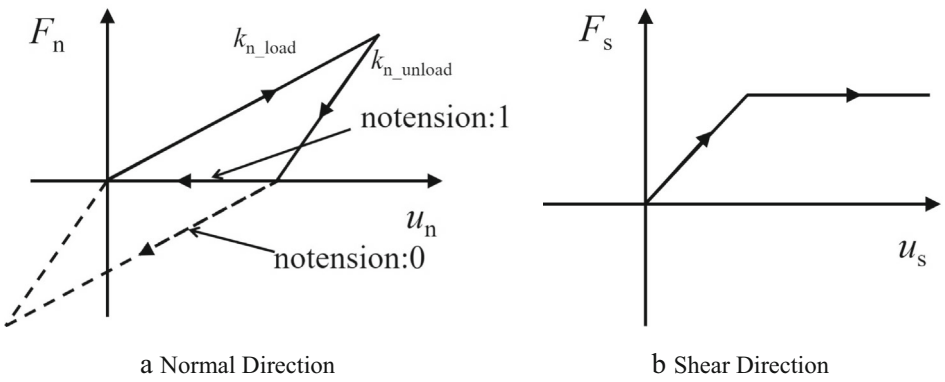

a Normal Direction b Shear Direction

Fig. 2 Hysteretic damping contact model

Table 1 Microscopic parameters of numerical model

	Ball	Wall	Tamper
Particle density/(kg m^{-3})	2650	–	1912
Normal stiffness k_n/(N m^{-1})	1.2e7	1e10	1e8
Shear stiffness k_s/(N m^{-1})	8e6	1e10	1e8
Friction coefficient	0.7	0	0.1

where k_0 is the initial normal stiffness, k_n, of particles under static loading, which was determined by numerical biaxial test; and R_h is the ratio of normal stiffness on loading, k_{n_load}, to that on unloading, k_{n_unload} ($0.05 < R_h < 1.0$). The dynamic hysteretic effect of soil is remarkable when R_h is close to 0, and R_h was determined to be 0.75 in this work according to a previous study (Jia et al. 2015).

3.2 Modeling

An axisymmetric numerical model for the sand sample adopted by Takada and Oshima centrifuge test (Takada and Oshima 1994) was established using PFC^{2D}. The tamper was modelled by 40 overlapping balls using the clump command in PFC^{2D}. The discrete element simulation of dry sand centrifugal test under DC has been carried out by Li et al. (2018), and the same microscopic parameters were adopted in this paper, as listed in Table 1. The generation method of the sample is the same to the literature (Li et al. 2018), and those particles, greater than 0.3 mm in diameter, were chosen to generate balls according to the proportion of particles in different ranges of particle size, as shown in Fig. 3 and Table 2 (S1). A vertical acceleration of 50 g was applied to each particle so that a centrifugal field could be obtained, thus a centrifuge test could be simulated. The time step was determined to be 1.0×10^{-6} s. The initial model and the model at 5000 steps are shown in Fig. 4, where the black line represents the force chain between particles.

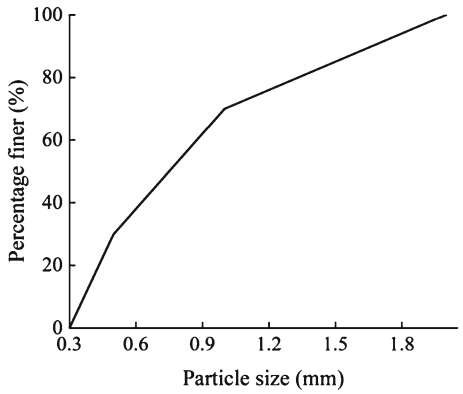

Fig. 3 Particle grading curve for Sample 1

To analyze the effect of grain gradation on the DC of dry sand, the models with different grain sizes were established. According to the field test compared with Takada and Oshima's centrifuge model test (Takada and Oshima 1994), the compression modulus of 5.05 MPa for the sand can be obtained (Li et al. 2018, 2021). The Poisson's ratio of dry sand was assumed to be 0.3. The microscopic parameters for the samples with different grading were obtained by calibrating the responses of biaxial test to achieve the results of the field test. The calibrated microscopic parameters by biaxial test are listed in Table 2, wherein sample 1 (denoted as S1) was generated by the gradation curve, and the particle diameters for mono-sized samples 2, 3 and 4 (denoted as S2, S3 and S4) are 2.0 mm, 1.0 mm and 0.3 mm, respectively. The porosity, Poisson's ratio and friction coefficient of these models are all 0.12, 0.3 and 0.7, respectively, which are the same as those in the reference (Li et al. 2018). The numbers of particles generated by S1, S2, S3 and S4 in DC simulations were 57,636, 5539, 21,975 and 242,800, respectively.

3.3 Layout of measurement circles

54 measurement circles, 0.012 m in radius, were arranged in numerical models, and the specific layout and numbering

Table 2 Parameters of specimens for biaxial test

	S1 (sample 1)	S2 (sample 2)	S3 (sample 3)	S4 (sample 4)
Particle diameter/(mm)	0.3–2.0	2.0	1.0	0.3
Model dimensions[a]/(m × m)	0.04 × 0.02	0.12 × 0.06	0.06 × 0.03	0.02 × 0.01
Particle number	2392	2016	2016	2489
Normal stiffness k_n/(N m^{-1})	1.2e7	8.2e6	8.0e6	8.5e6
Shear stiffness k_s/(N m^{-1})	8.0e6	5.0e6	5.0e6	5.0e6

[a]Model dimensions are denoted as height × width

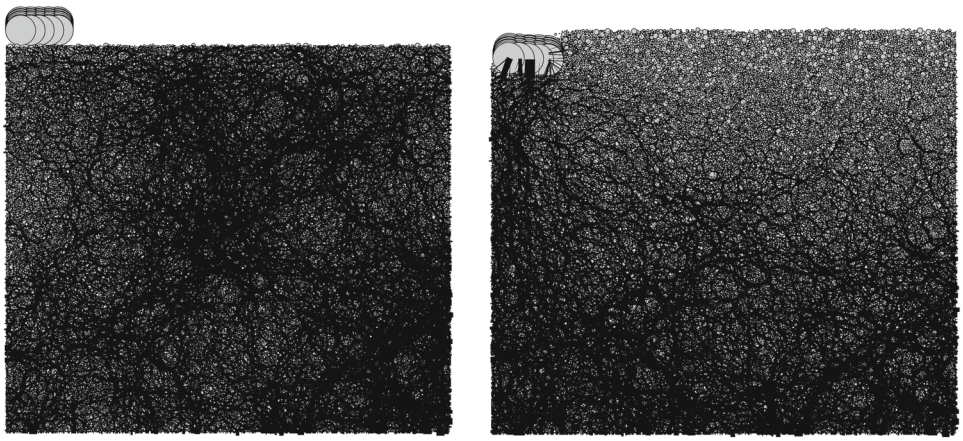

Fig. 4 Discrete element model

a Initial model b The model at 5000 steps

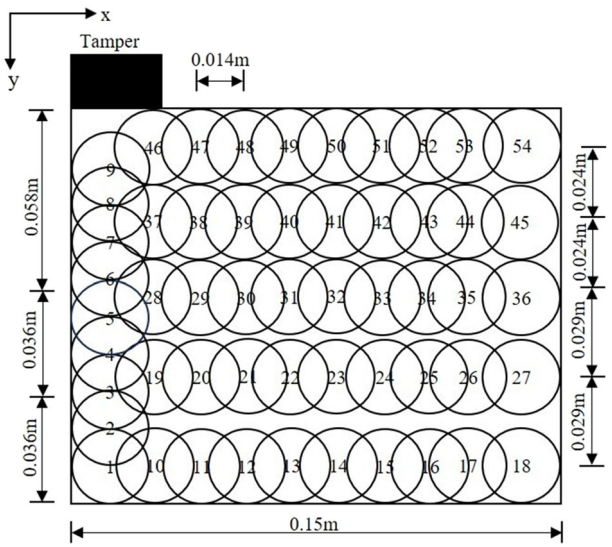

Fig. 5 Layout and numbering of measurement circles

are shown in Fig. 5. The measurement circles 6 and 3, which correspond to 2.9 m and 4.7 m below the ground surface, were selected to investigate the influence of grain size on the micro characteristics of soil under DC.

4 Results and analysis

4.1 Propagation of dynamic contact stress

According to the data attained from the measurement circles 6 and 3, the time histories of vertical contact stress can be plotted, as shown in Fig. 6. It is indicated in Fig. 6 that the time histories of contact stress with different particle gradation under dynamic load were all single peak curves. The closer the measurement circle was to the tamping point, the earlier the stress wave arrived, and the earlier the stress reached the peak value. The vertical stresses reached to the peak value at 0.2 s and attenuated at about 0.3 s. As the depth of test points increased, the difference in stress peak between the mono-sized samples (S2, S3 and S4) and the sample (S1) generated by the gradation curve became small since the influence of DC became small and gravity became large. It can also be seen from Fig. 6 that the peak values of the vertical stress for the mono-sized samples were smaller than those for the sample generated by the gradation curve. Also, the smaller the particle size was, the smaller the stress peak was (Wu et al. 2017). With the increase in the depth of test points, the influence of grain size on the peak of vertical stress became small, as shown in Fig. 6b. Therefore, the dynamic stress response for the sample (S1) generated by the gradation curve was larger under the same dynamic load, i.e., the variation of stress increase and attenuation was greater within the same

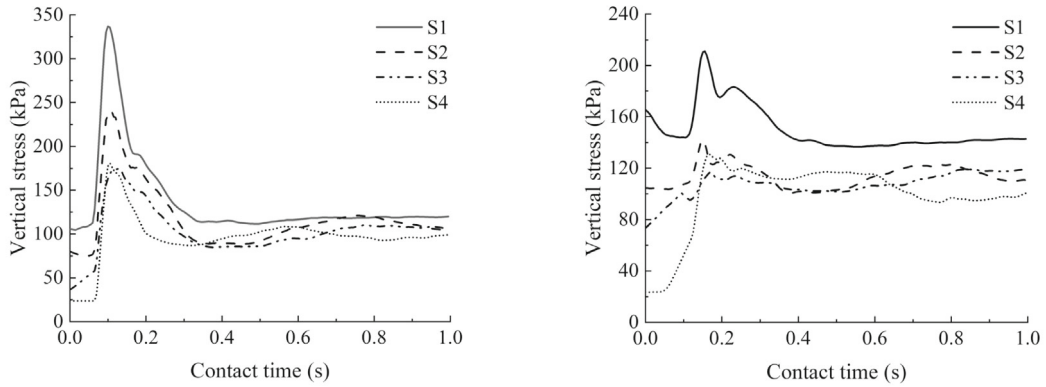

Fig. 6 Time histories of vertical stress at different depths

time, which demonstrates that the better the particle gradation was, the better the effect of force transfer was. When choosing the foundation treatment parameters of DC, attention should be paid to particle size distribution and particle size of site soil.

4.2 Coordination number

Coordination number, defined as the average number of contacts per particle (Itasca Consulting Group 2004; Kodicherla et al. 2020), can measure the intensity of packing. The time histories of average coordination number of particles are shown in Fig. 7, which was in accord with the results of the indoor DC model test (Jia et al. 2009). Under impact load, the increase in the coordination number of particles indicates that the soil particles became dense. The curve of particle coordination number included three stages, that was, rising, decreasing and stabilizing. Figure 7 displays that the coordination numbers of particles for the sample (S1) generated by the particle size distribution were smaller than those of mono-sized samples, and the difference became larger with the increase in the depth of test points. This conclusion also further highlights the one drawn by Ueda et al. (2012) through numerical tests that the standard deviation of particle size was large, i.e., the gradation was good, and the coordinate number was small. Since the initial porosity of the model was constant, the better the gradation was, the more uneven the particle size was. The coordination number increased because the small-sized particles more sufficiently contacted with those particles with large size after DC. As to the mono-sized specimen, since the particle was assumed to be a disk and their size was the same, the sample was difficult to become dense under DC. With the increase in depth, the impact effect of DC on soil became weak, and hence the change of coordination number also became very small. Therefore, the poorly graded soil is more difficult to treat, especially under the assumption of 2D disk, which is consistent with engineering practice.

4.3 Porosity

Porosity is defined as the ratio of total void area within the measurement circle to measurement circle area (Itasca Consulting Group 2004). Figure 8 shows the time histories of porosity at the measurement circles 6 and 3, respectively. As it can be seen from Fig. 8, the porosities were almost unchanged at the beginning, then decreased rapidly, then rebounded and eventually became stable, and the porosities after the stabilization were smaller than the initial values. For the well-graded sample (S1), when the coarse particles were dominant, the fine particles would fill the voids between the coarse particles. However, some isolated fine particles might be trapped in the narrow gaps between the coarse particles, thus causing the wedging effect (Kwan et al. 2013). Therefore, the final porosity for the sample (S1) generated by the particle size distribution was the largest and the porosity for the sample (S3) with the diameter of 1.0 mm was the smallest.

As mentioned above and shown in Fig. 8, the variation of porosity was insignificant at the initial stage. The deeper the measurement point was, the longer the duration at this stage was, as the result of gradual deepening of stress wave transmission. Therefore, there was a certain time delay in the compaction process of soil with the increase in depth. After the initial stage, the porosity curves for the samples all experienced a process of rapid decrease, rebound and stabilization no matter what particle size distribution was, which indicates that soil samples all became denser. In addition, as the depth of measurement point increased, the peak value of vertical stress (see Fig. 6b) became small, and the valley values of porosity all decreased, i.e. they were greater, regardless of particle size distribution. Hence, the influence of DC on soil became small with the increase in depth.

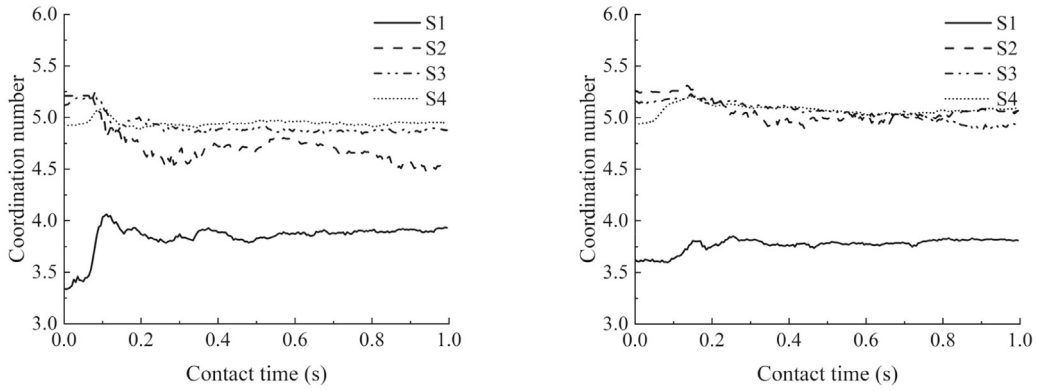

a Measurement circle 6 (2.9 m) b Measurement circle 3 (4.7 m)

Fig. 7 Time histories of coordination numbers at different depths

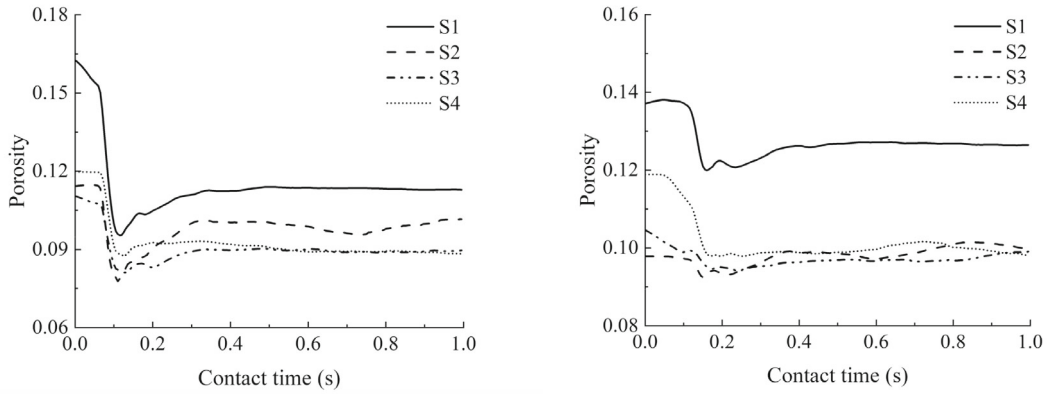

a Measurement circle 6 (2.9 m) b Measurement circle 3 (4.7 m)

Fig. 8 Time histories of porosity at different depths

Table 3 Change rate of porosity after dynamic compaction

	Measurement circle 6 (2.9 m) (%)	Measurement circle 3 (4.7 m) (%)
S1	− 30.58	− 7.72
S2	− 12.12	3.03
S3	− 19.11	− 5.99
S4	− 25.85	− 16.78

The porosity variation of the samples before and after tamping is listed in Table 3. It can be seen from Table 3 that there was a satisfactory compaction effect at the measurement circle 6. At 4.7 m (Measurement circle 3) below ground surface, the change rate of porosity was small, especially for the soil specimen with poor gradation or larger particle size, which further illustrated the effective reinforcement depth of about 5.0 m under current energy level.

4.4 Crater depth

When the energy is applied to each impact point of ground surface, the most obvious manifestations of subsidence are the relatively large craters (Mayne et al. 1984). The depth of these craters is called crater depth. The crater depth is related to the energy per blow, the number of blows, and the type of soil (Mayne et al. 1984). Figure 9 shows the relationship between the crater depth and the number of blows for specimens with different particle gradations, which was consistent with the previous studies (Takada and Oshima 1994; Gu and Lee 2002). The relationship between the crater depth and the number of blows for the specimen generated by the gradation curve has been reported and validated with the results of centrifuge test and field test (Li et al. 2018). As shown in Fig. 9, the crater depth at the first blow was the largest, and with the increase in tamping time, the crater depth of each blow decreased as a result of the compaction of soil (Jia et al.

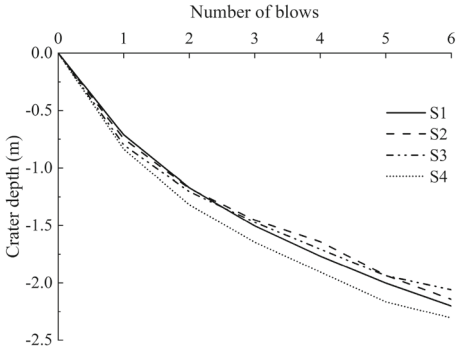

Fig. 9 Variation of crater depth with the number of blows

2009; Li et al. 2018). The settlement values for the mono-sized samples of 2.0 mm (S2) and 1.0 mm (S3) in diameter were almost the same as those for the sample generated by the gradation curve (S1), especially at the first three tamping. However, the settlement values for the mono-sized sample of 0.3 mm (S4) in diameter were larger. According to Table 3, at 4.7 m below the ground surface, the change rate of porosity for the mono-sized sample of 0.3 mm in diameter was still 16.78%, thus the sample was compressed more closely, and the settlement values were greater.

5 Conclusions

Due to few studies on the microscopic behavior of soil under DC, the models for DC of dry sand with different particle size distributions were established using the hysteretic damping model in PFC^{2D}. The investigation of the effect of particle gradation on soil stress, coordination number, porosity and crater depth at a particle level is helpful to understand the microscopic mechanism of soil compaction and can guide the construction of DC. The following conclusions were drawn:

1. The final stress and porosity for the sample generated by the gradation curve were the largest, whereas its coordination number was the smallest.
2. The change rates of stress, coordination number and porosity of the sample generated by the gradation curve were greater than the results from the mono-sized samples. Therefore, the better the particle gradation was, the better the effect of force transfer was and the better the compaction was.
3. The influence depth of the sample generated by the gradation curve on stress and porosity was large; however, its effect on the coordination number was relatively shallow.
4. For a mono-sized sample and a well-graded sample, the differences in stress, coordination number and porosity of soil increased with the increase in depth.

Author contributions Y. Li, L. Xu and F. Yang performed the numerical simulations and wrote the main manuscript text. All authors reviewed the manuscript.

Data availability All data, models and code that support the findings of this study are available from the corresponding author upon reasonable request.

Declarations

Conflict of interest On behalf of all authors, the corresponding author states that there are no competing interests to declare.

References

Chow YK, Yong DM, Yong KY, Lee SL (1992) Dynamic compaction of loose sand deposits. Soils Found 32(4):93–106

Fang Q, Zhang J, Zhang Y, Liu J (2016) Mesoscopic investigation of the sand particulate system subjected to intense dynamic loadings. Int J Impact Eng 89:62–71

Feng TW, Chen KH, Su YT, Shi YC (2000) Laboratory investigation of efficiency of conical-based pounders for dynamic compaction. Geotechnique 50(6):667–674

Ghassemi A, Pak A, Shahir H (2010) Numerical study of the coupled hydro-mechanical effects in dynamic compaction of saturated granular soils. Comput Geotech 37:10–24

Gu Q, Lee FH (2002) Ground response to dynamic compaction of dry sand. Geotechnique 52(7):481–493

Gu X, Lu L, Qian J (2017) Discrete element modeling of the effect of particle size distribution on the small strain stiffness of granular soils. Particuology 32:21–29

Hu RL, Yeung MR, Lee CF, Wang SJ (2001) Mechanical behavior and microstructural variation of loess under dynamic compaction. Eng Geol 59:203–217

Hwang JH, Tu TY (2006) Ground vibration due to dynamic compaction. Soil Dyn Earthq Eng 26:337–346

Itasca Consulting Group (2004) Particle flow code in 2 dimensions (Version 3.1). Itasca Consulting Group Inc., Minneapolis

Jia M, Wang L, Zhou J (2009) Experimental research on macro-meso consolidation mechanism of sandy soil with dynamic compaction. Chin J Rock Mech Eng 28(Supp. 1):3282–3290

Jia M, Wu S, Ye J (2015) Discrete element modeling of dynamic compaction in granular soils using PFC3D. J Hunan Univ (natural Sciences) 42(3):70–76

Jiang M, Wu D, Xi B (2017) DEM simulation of dynamic compaction with different tamping energy and calibrated damping parameters. In: Li X, Feng Y, Mustoe G (eds) Proceedings of the 7th international conference on discrete element methods. Springer, Singapore, pp 845–851

Kodicherla SPK, Gong G, Moy CKS, Fan L, Kristian K (2020) Direct shear test simulations using DEM. In: Latha GM, Raghuveer RP (eds) Lecture notes in civil engineering: geotechnical characterization and modelling. Springer, Singapore, pp 849–855

Kwan AKH, Chan KW, Wong V (2013) A 3-parameter particle packing model incorporating the wedging effect. Powder Technol 237:172–179

Lee FH, Gu Q (2004) Method for estimating dynamic compaction effect on sand. J Geotech Geoenviron Eng 130(2):139–152

Li Y, Chen J, Chen X (2018) Discrete element simulation of centrifuge test of dry sand under dynamic compaction. In: Zhou A, Tao J, Gu X and Hu L (eds) Proceedings of GeoShanghai 2018 international conference: fundamentals of soil behaviours. Springer, Singapore, pp 819–825

Li Y, Zhang J, Chen J, Chen X, Zhang W (2021) A micro study on centrifuge model test of dynamic compaction using discrete element method. Proc Inst Civ Eng Geotech Eng 174(5):488–497

Liu P, Yu Q, Zhao X, Zhou C, Shi P (2020) Three-dimensional discrete element modeling of the irregularly shaped pebbles used in a truck escape ramp. Comput Part Mech 7(3):479–490

Lu H, Luo H, Cooper WL, Komanduri R (2013) Effect of particle size on the compressive behavior of dry sand under confinement at high strain rates. In: Chalivendra V, Song B, Casem D (eds) Proceedings of the 2012 annual conference on experimental and applied mechanics: dynamic behavior of materials, vol 1. Springer, New York, pp 523–530

Lukas RG (1980) Densification of loose deposits by pounding. J Geotech Geoenviron Eng 106(4):435–446

Luo H, Cooper WL, Lu H (2014) Effects of particle size and moisture on the compressive behavior of dense Eglin sand under confinement at high strain rates. Int J Impact Eng 65:62–71

Ma ZY, Dang FN, Liao HJ (2014) Numerical study of the dynamic compaction of gravel soil ground using the discrete element method. Granul Matter 16:881–889

Mayne PW, Jones JS, Dumas JC (1984) Ground response to dynamic compaction. J Geotech Eng 110(6):757–774

Miao LC, Chen G, Hong ZS (2006) Application of dynamic compaction in highway: a case study. Geotech Geol Eng 24:91–99

Pan JL, Selby AR (2002) Simulation of dynamic compaction of loose granular soils. Adv Eng Softw 33:631–640

Poran CJ, Rodriguez JA (1992) Finite element analysis of impact behavior of sand. Soils Found 32(4):68–80

Takada N, Oshima A (1994) Comparison between field and centrifuge model tests of heavy tamping. In: Leung CF, Lee FH, Tan TS (eds) Proceedings of the international conference centrifuge 94. Balkema AA, Rotterdam, pp 337–342

Thilakasiri HS, Gunaratne M, Mullins G, Stinnette P, Jory B (1996) Investigation of impact stresses induced in laboratory dynamic compaction of soft soils. Int J Numer Anal Meth Geomech 20:753–767

Ueda T, Matsushima T, Yamada Y (2012) Micro structures of granular materials with various grain size distributions. Powder Technol 217:533–539

Wang W, Chen JJ, Wang JH (2017) Estimation method for ground deformation of granular soils caused by dynamic compaction. Soil Dyn Earthq Eng 92:266–278

Wu K, Rémond S, Abriak N, Pizette P, Becquart F, Liu S (2017) Study of the shear behavior of binary granular materials by DEM simulations and experimental triaxial tests. Adv Powder Technol 28:2198–2210

Xie N, Ye Y, Wang L (2013) Numerical analysis of dynamic contact during dynamic compaction with large deformation. J Eng Mech 139(4):479–488